

Boron dipyrdimethene (DIPYR) dyes: shedding light on pyridine-based chromophores

Jessica H. Golden, John W. Facendola, Daniel Sylvinson, Cecilia
Quintana Baez, Peter I. Djurovich, and Mark E Thompson

J. Org. Chem., **Just Accepted Manuscript** • DOI: 10.1021/acs.joc.7b00786 • Publication Date (Web): 04 Jul 2017

Downloaded from <http://pubs.acs.org> on July 4, 2017

Just Accepted

"Just Accepted" manuscripts have been peer-reviewed and accepted for publication. They are posted online prior to technical editing, formatting for publication and author proofing. The American Chemical Society provides "Just Accepted" as a free service to the research community to expedite the dissemination of scientific material as soon as possible after acceptance. "Just Accepted" manuscripts appear in full in PDF format accompanied by an HTML abstract. "Just Accepted" manuscripts have been fully peer reviewed, but should not be considered the official version of record. They are accessible to all readers and citable by the Digital Object Identifier (DOI®). "Just Accepted" is an optional service offered to authors. Therefore, the "Just Accepted" Web site may not include all articles that will be published in the journal. After a manuscript is technically edited and formatted, it will be removed from the "Just Accepted" Web site and published as an ASAP article. Note that technical editing may introduce minor changes to the manuscript text and/or graphics which could affect content, and all legal disclaimers and ethical guidelines that apply to the journal pertain. ACS cannot be held responsible for errors or consequences arising from the use of information contained in these "Just Accepted" manuscripts.



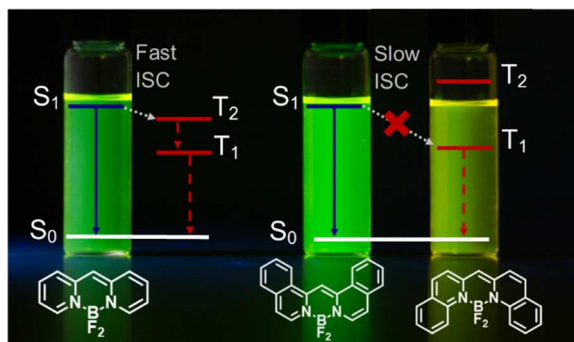
Boron dipyridylmethene (DIPYR) dyes: shedding light on pyridine-based chromophores

Jessica H. Golden,[†] John W. Facendola,[†] Daniel Sylvinson M. R.,[†] Cecilia Quintana Baez,[‡]

Peter I. Djurovich,[†] and Mark E. Thompson^{*,†,‡}

Department of Chemistry[†] and Mork Family Department of Chemical Engineering and Materials
Science[‡], University of Southern California, Los Angeles, California, 90089, United States

FOR TABLE OF CONTENTS ONLY



ABSTRACT:

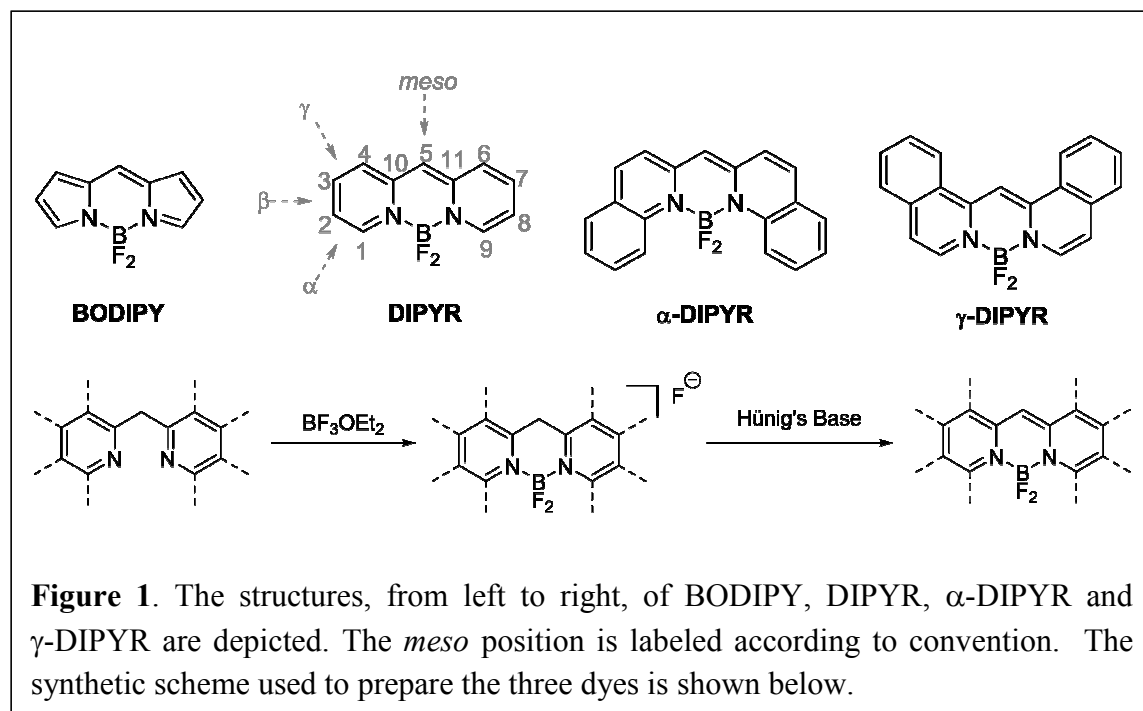
Boron dipyrromethenes (BODIPY) derivatives have found widespread utility as chromophores in fluorescent applications, but little is known about the photophysical properties of pyridine-based BODIPY analogues, dipyridylmethene dyes. Indeed, it has been reported that boron difluoride dipyridylmethene (DIPYR) is non-emissive, and that derivatives of DIPYR have modest, if any, luminescence. In this report, we explore this little-touched area of chemical space and investigate the photophysical properties of three simple DIPYR dyes: boron dipyridylmethene, boron diquinolymethene, and boron diisquinolymethene. The three dyes absorb strongly in the blue-

green part of the spectrum ($\lambda_{\text{em}} = 450\text{--}520\text{ nm}$, $\epsilon = 2.9\text{--}11 \times 10^4\text{ M}^{-1}\text{cm}^{-1}$) and display green fluorescence with high quantum yields ($\Phi_{\text{PL}} = 0.2, 0.8$ and 0.8 , respectively). Key photophysical properties in these systems were evaluated using a combination of TD-DFT and extended multi-configurational quasi-degenerate second order perturbation theory (XMCQDPT2) methods and compared to experiment, revealing that high quantum yields of the quinoline and isoquinoline derivatives are a result of the relative reordering of S_1 and T_2 state energies upon benzannulation of the parent structure. The intense absorption and high emission efficiency of the benzannulated derivatives make these compounds an intriguing class of dyes for further derivatization.

INTRODUCTION:

The boron dipyrromethene (BODIPY) core structure is pervasive among fluorescent dyes employed in biological and optoelectronic applications. BODIPYs have been utilized in protein and DNA labeling,¹⁻⁵ as fluorescent switches and chemosensors,⁶⁻⁸ as laser dyes,⁹ and in photovoltaics.^{10,11} Their physical and photophysical properties can be readily tuned by making simple substitutions on the pyrroles or at the *meso* position, and they tend to have little dependence on solvent polarity or pH, which makes them ideal fluorophores for *in vivo* labeling.¹² These features, along with a high luminance efficiency and photostability, have led to the popularity of BODIPY compounds. Despite the wide landscape of BODIPY dyes available, further investigation into the derivatization of BODIPYs and the development of alternative fluorescent dyes remains an active area of research due to specific limitations presented by BODIPYs.¹³ Indeed, some simple synthetic modifications of BODIPYs have proven challenging; for example, although the class of dyes has been known since 1968, it was not until 2009 that the parent structure was successfully isolated.¹⁴⁻¹⁶ Given the enormous body of work available on the derivatization and application of BODIPYs and related fluorophores, we found it surprising that very little research has been reported on the photophysical properties of pyridine-based BODIPY-like dyes.

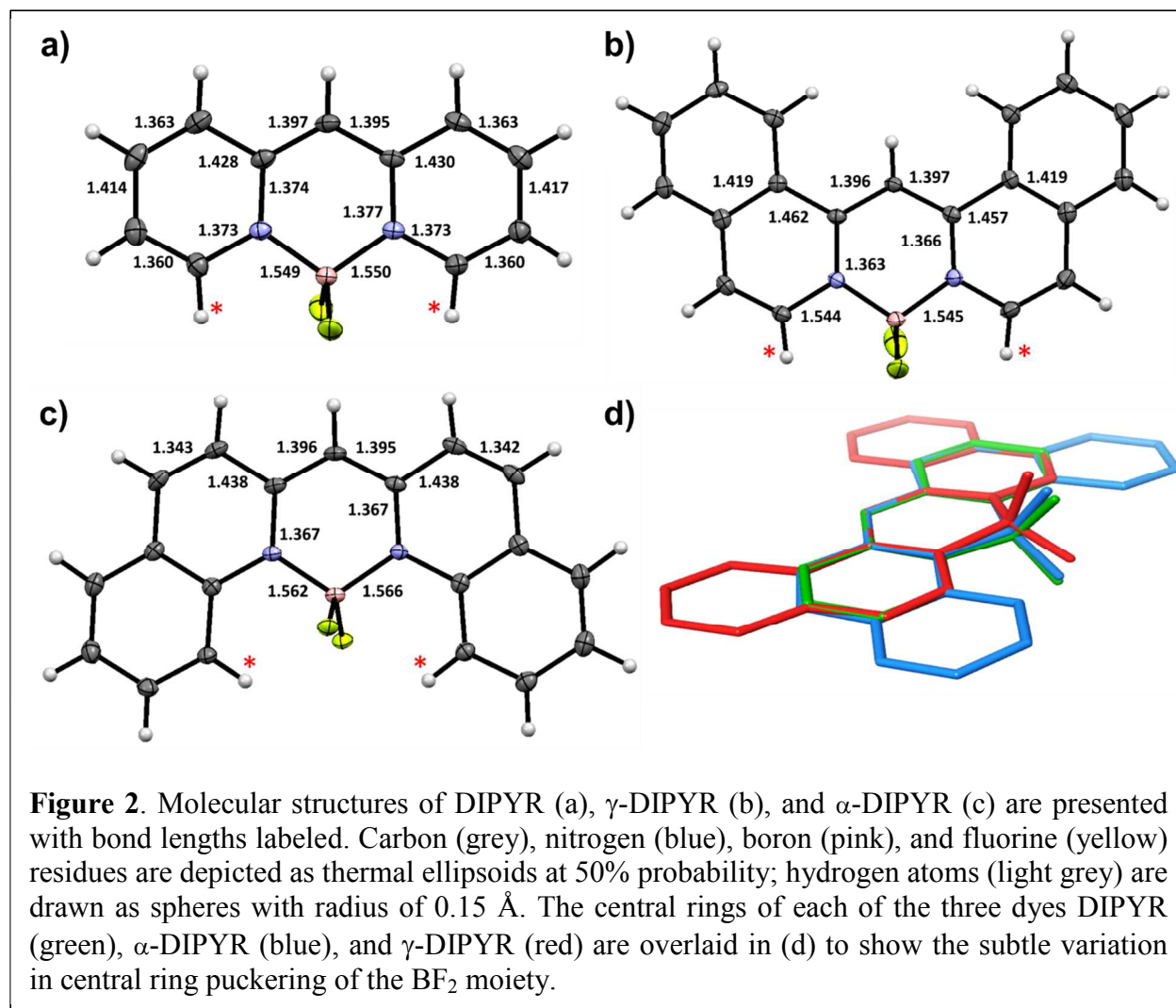
In this work we aim to expand the scope of BODIPY-like dyes by the replacement of the pyrroles in BODIPY with pyridine moieties. The resultant class of boron difluoride dipyritylmethene (DIPYR) fluorescent dyes (Figure 1) are similar in geometric structure to anthracene and dibenz[*a,j*]anthracene, and superficially appear to be a mix between acenes and BODIPYs. Considering their intriguing combination of structural features, it is therefore somewhat surprising that only a handful of studies have appeared regarding the photophysical properties for this class of compounds. For example, the first report on the preparation of DIPYR in 1973 made no mention of luminescent properties,¹⁷ while a later paper describing the photophysical properties of the related boron dipyritylamine dyes incorrectly described DIPYR as being non-emissive.¹⁸ It is likely for this reason that follow-up research on this class of dye molecules has been limited.¹⁹ However, dipyritylamine analogues of DIPYR dyes with nitrogen at the *meso* position do display UV-violet emission ($\lambda_{\text{em}} = 362\text{--}416\text{ nm}$) and have luminescent quantum yields ($\Phi_{\text{PL}} = 0.4$)¹⁸ similar to values found for the blue-emissive *meso*-cyano substituted DIPYR dyes ($\lambda = 450\text{ nm}$, $\Phi_{\text{PL}} = 0.2$).¹⁹ These promising photophysical properties piqued our interest in the study of the parent DIPYR dyes with methine at the *meso* position. Herein we report the synthesis, structural and photophysical properties of this promising new family of pyridine-, quinoline-, and isoquinoline-derived fluorescent dyes. We find that benzannulation of DIPYR leads to higher absorptivity and substantial increases in luminescent efficiency, with quantum yields ($\Phi_{\text{PL}} = 0.8$) that approach values comparable to the most highly efficient BODIPY dyes. The increase in fluorescent efficiency in the quinoline and isoquinoline DIPYR derivatives is attributed to a decrease in the rate of intersystem crossing caused by a change in energetic ordering of the S_1 and T_2 excited states.



RESULTS & DISCUSSION:

The methylene-bridged heteroaryl precursors to DIPYR dyes were prepared according to literature procedures.^{20,21} The synthetic route to DIPYR dyes (Figure 1) involves first borylating the diheteroaryl methane ligand by refluxing in the presence of boron trifluoride diethyl etherate, to prepare a fluoride salt which precipitates from the reaction mixture upon cooling. The salt is then deprotonated with an excess of Hünig's base to produce the final product in 38% yield. This method is similar to one used to obtain *meso*-cyano DIPYRs,¹⁹ and was also used to prepare α -DIPYR and γ -DIPYR in 39% and 36% yields, respectively. It is interesting to note that in the case of dipyridylamine ligands, the deprotonation step occurs without the need for addition of base. The early report,¹⁸ comparing DIPYR (methane-bridged) with dipyridylamine (nitrogen-bridged) analogues, did not include a deprotonation step, and thus isolation of the intermediate salt *in lieu* of DIPYR itself may be the source of confusion in the literature regarding the emissive properties of DIPYR dyes.

Molecular structures of DIPYR, γ -DIPYR, and α -DIPYR obtained by X-ray diffraction analysis are shown in Figure 2 (crystal packing figures are available in the SI). The carbon–carbon bonds of DIPYR mimic a pattern of alternating short (C1–C2 and C3–C4) and long (C2–C3 and C4–C5) distances similar to that found in the aromatic rings of anthracene.²² An intermediate distance to the *meso*-carbon (C5–C6) is also found for the related C–C bond in anthracene. The carbon–nitrogen bond distances (C1–N1 and C5–N1) are elongated relative to the values found in pyridine (C–N = 1.337 Å) and more closely correspond to the elongated C–C bond lengths for the equivalent atom positions in anthracene. This bond length alternation pattern is preserved in the benzannulated derivatives, although the distances between the bridging C–C atoms are lengthened relative to those of the parent structure. A narrow range for the boron–nitrogen (1.544–1.566 Å) and boron–fluorine (1.390–1.404 Å) bond lengths in all three derivatives indicates closely related bonding interactions between these atoms. Interestingly, in all three compounds the central six-membered borocyclic ring adopts a boat-like confirmation, wherein the BF₂ moiety and *meso*-carbon lie above the plane of the central ring, with the BF₂ group residing further out of plane (Figure 2d). The distance to which the BF₂ moiety is out-of-plane (d_{op}) is larger in γ -DIPYR (d_{op} = 0.23 Å) than in either DIPYR (d_{op} = 0.09 Å) or α -DIPYR (d_{op} = 0.04 Å). Although γ -DIPYR exhibits a larger distortion relative to the other two DIPYRs, the small deviation from planarity in the borocyclic ring may be simply a result of crystal packing forces.



It is useful to compare the structural characteristics of the DIPYR dyes to analogous BODIPY dyes. The variation in C–C bond lengths in the five-membered ring of BODIPY is smaller (1.370–1.410 Å)¹⁴ than in DIPYR (1.360–1.430 Å), suggesting a greater degree of cyanine-like interaction between the canonical resonance structures of BODIPY than of DIPYR. Bond distances between B–N and B–F are comparable in both types of chromophores, and both exhibit slight puckering of the boron atom out of the plane of the borocyclic ring ($d_{\text{op}} = 0.146$ Å in BODIPY and 0.09 Å in DIPYR). One significant difference between BODIPY and the DIPYR derivatives is the average distance between the fluorine atoms and the nearest hydrogen

atoms (Figure 2, starred, for DIPYRs). The closest intramolecular H \cdots F distances in the parent BODIPY (3.0 Å) fall outside the Van der Waal radii of the two atoms (2.67 Å).²³ In contrast, the equivalent protons in DIPYRs are positioned much closer to the fluorine atoms; the shortest intramolecular H \cdots F distances found in DIPYR and γ -DIPYR are 2.55 Å and 2.43 Å, respectively, whereas the benzannulated rings of α -DIPYR place the atoms in even closer proximity (H \cdots F = 2.34 to 2.49 Å). The effect of the short H \cdots F distances is manifested in the coupling of the ^1H NMR resonances at these positions. The doublets in DIPYR (δ = 7.90 ppm, $^3J_{\text{HH}}$ = 5.5 Hz) and γ -DIPYR (δ = 7.88 ppm, $^3J_{\text{HH}}$ = 7.0 Hz) are broadened due to through-space coupling to the ^{19}F atoms,²⁴ and the corresponding protons in α -DIPYR (δ = 8.57 ppm) are clearly resolved into a doublet of triplets ($^3J_{\text{HH}}$ = 8.8 Hz, $^4J_{\text{FH}}$ = 3.5 Hz).

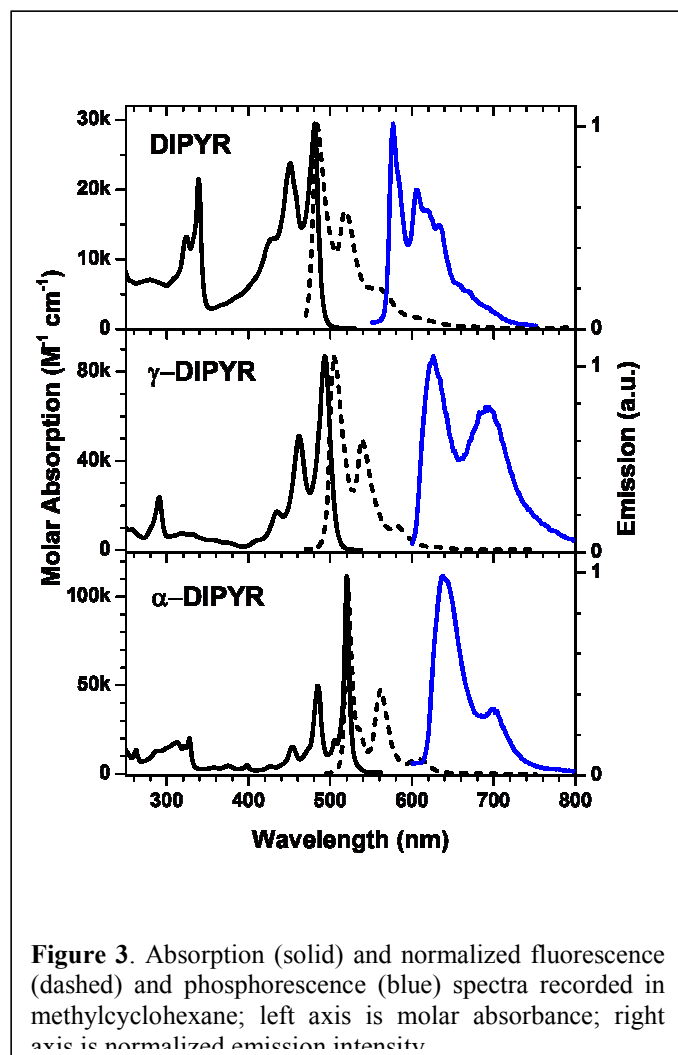
The electrochemical properties of the dyes were examined using cyclic voltammetry (Figures S3-S5); redox potentials versus an internal ferrocene standard are given in Table 1. The oxidation waves in all three materials are irreversible. The reduction wave in DIPYR is quasi-reversible, while waves in both α -DIPYR and γ -DIPYR are reversible. The irreversible oxidation in DIPYR dyes may be the result of the coupling of two oxidized molecules, a phenomenon which has been observed during the oxidation of BODIPYs and cyanines.²⁵⁻²⁸ Oxidation of DIPYR occurs at a much lower potential (E_{ox} = 0.14 V) than in BODIPY (E_{ox} = 1.35 V),²⁹ whereas the reduction potential is correspondingly more negative (DIPYR, E_{red} = -2.32 V; BODIPY, E_{red} = -1.05 V).^{28,30} The redox potentials of both α -DIPYR and γ -DIPYR are anodically shifted relative to the parent compound indicating stabilization of both valence MOs upon benzannulation, with the LUMO stabilized to a greater degree than the HOMO.

Table 1. Redox potentials (V vs. Fc^+/Fc)^a

	E_{ox}	E_{red}	ΔE_{redox}
DIPYR	0.14	-2.32	2.48
α -DIPYR	0.40	-1.95	2.35
γ -DIPYR	0.27	-2.07	2.34

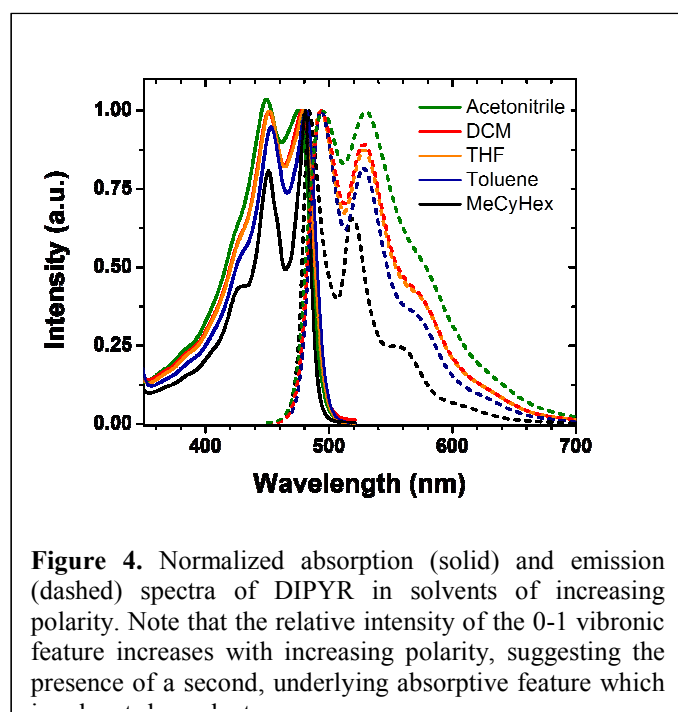
^aIn acetonitrile with 0.1 M TBAF.

The photophysical properties of the dyes were characterized using UV-visible absorption and emission spectroscopies (Figure 3); data are summarized in Table 2. All of the DIPYRs display intense ($\epsilon > 10^4 \text{ M}^{-1}\text{cm}^{-1}$), vibronically structured absorption bands in the UV-visible spectrum. The lineshape of the DIPYR absorbance band is similar to the profile reported for *meso*-cyano DIPYR.¹⁹ The lowest energy absorption bands become more intense and red-shift in the benzannulated derivatives. The vibronic manifolds display major progressions of 1475 cm^{-1} , similar to the spacings found in anthracene, and the 0-0 transitions become stronger and more intense than the 0-1 transitions in the benzannulated derivatives. The lowest absorption transitions in all derivatives display small hypsochromic shifts ($< 10 \text{ nm}$) in going from non-polar (methylcyclohexane) to polar (acetonitrile) solution.



Interestingly, the absorption lineshape of DIPYR is solvent dependent; the 0-1 peak of the vibronic progression gradually increases in intensity with increasing solvent polarity, becoming more intense than the 0-0 transition in acetonitrile solution (Figure 4). In contrast, aside from an increase in the inhomogeneous broadening in acetonitrile, the absorption lineshapes for α -DIPYR and γ -DIPYR are similar in both solvents. The change in the lineshape with solvent polarity for DIPYR suggests the presence of a second, weaker transition lying at a slightly higher energy than the S_0 - S_1 transition. This supposition is supported by theoretical calculations of the excited state (*vide infra*). Another notable feature in the absorption spectra is an extremely

narrow linewidth for the 0-0 transition of α -DIPYR, which has a full width half-maximum (fwhm) of 250 cm^{-1} . This transition is much narrower than the 0-0 transition in γ -DIPYR (fwhm = 700 cm^{-1}) and even less than the value found for the corresponding feature of anthracene (fwhm = 440 cm^{-1}). The narrow linewidth for the 0-0 transition, along with the large ratio between the 0-0 and 0-1 transitions, indicate that there is minimal structural distortion in the excited state of α -DIPYR.



All of the DIPYR derivatives are highly luminescent in solution and display small Stokes shifts ($< 5\text{ nm}$) in non-polar solvents. A noticeable asymmetry is present in the mirror image relationship between absorption and emission in DIPYR, consistent with the absorption profile being distorted by an S_2 state lying at slightly higher energy than the S_1 state. In contrast, the absorption and emission spectra of the benzannulated derivatives display a near perfect mirror symmetry. DIPYR has a photoluminescent quantum yield (Φ_{PL}) of 17% in methylcyclohexane

and 8.5% in acetonitrile, whereas the values for α - and γ -DIPYR are much higher ($\Phi_{\text{PL}} = 77\%$ and 80%, respectively) and nearly solvent independent. The radiative rate constants (k_r) are similar in value among all three derivatives ($k_r = 0.91\text{--}2.0 \times 10^8 \text{ s}^{-1}$), whereas the rate for non-radiative decay (k_{nr}) of DIPYR in methylcyclohexane ($k_{\text{nr}} = 4.5 \times 10^9 \text{ s}^{-1}$) is nearly two orders of magnitude larger than values for α - and γ -DIPYR ($k_{\text{nr}} \approx 4.5 \times 10^7 \text{ s}^{-1}$). The notably faster rate for non-radiative decay in DIPYR is not the result of structural distortions in the excited state as no major change in the luminescent lifetimes (τ) occurs in either fluid solution at room temperature ($\tau = 1.9 \text{ ns}$) or rigid media at 77 K ($\tau = 2.0 \text{ ns}$). A more plausible explanation for the large k_{nr} value of DIPYR is a fast rate for intersystem crossing (ISC) between singlet and triplet states. Support for this mechanistic hypothesis is based on the fact that phosphorescent emission ($E_{0-0} = 577 \text{ nm}$) is readily observed in the parent DIPYR in frozen methylcyclohexane at 77 K, whereas none is observed under similar conditions for α - and γ -DIPYR. It is possible, however, to record phosphorescence from the benzannulated compounds in frozen solutions using more rigorous conditions of gated detection, along with the addition of iodomethane to promote ISC through an external heavy atom effect (Figure 3).

Table 2. Photophysical properties of DIPYR dyes^a

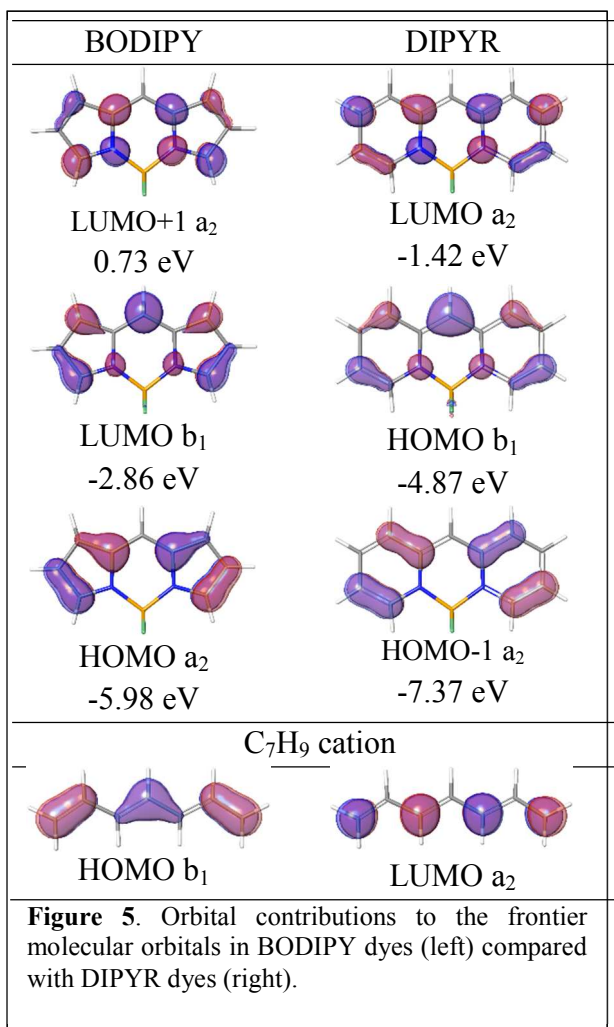
	absorption λ_{max} (nm)	ϵ ($\text{M}^{-1}\text{cm}^{-1}$)	emission λ_{max} (nm)	Φ_{PL}	τ (ns)	k_r (10^8 s^{-1})	k_{nr} (10^8 s^{-1})
DIPYR	481 (476)	2.9×10^4	484 (496) 482 ^b , 577 ^c	0.17 (0.085)	1.9 (1.6) 2.0 ^b	0.91(0.53)	4.5 (5.7)
α -DIPYR	520 (515)	1.1×10^5	520 (521) 520 ^b , 638 ^c	0.77 (0.77)	5.7 (5.0) 4.7 ^b	1.4 (1.5)	0.41 (0.46)
γ -DIPYR	500 (493)	8.7×10^4	504 (504) 504 ^b , 626 ^c	0.80 (0.75)	3.9 (4.1) 3.6 ^b	2.0 (1.8)	0.51 (0.61)

^aMeasurements acquired at room temperature in methylcyclohexane (acetonitrile). ^bFluorescence and ^cphosphorescence at 77 K in methylcyclohexane.

The electronic characteristics of DIPYR dyes in the gas phase were examined using both time-dependent density functional (TD-DFT) and extended multi-configurational quasi-

degenerate second order perturbation (XMCQDPT2)³¹ theoretical calculations (see SI for a thorough analysis of computational methods). The XMCQDPT2 calculations were employed on account of recent studies where it has been determined that optical transitions in *meso*-cyano DIPYR and related cyanine-type dyes are multireference in nature and are accompanied by a significant double excitation character in their excited states.³² Singlet excitation energies calculated for these pseudo-aromatic dyes using single reference methods such as TD-DFT are found to have errors greater than 0.3 eV.^{32,33} However, despite the large absolute errors, the calculated TD-DFT values for this class of molecules can be scaled linearly with experimental excitation energies.³³

The DFT calculations replicate the pattern of C–C and C–N bond length alternation found in the X-ray structures of the molecules, including an out-of-plane distortion ($d_{op} = 0.42 \text{ \AA}$) of the BF_2 group in the six-membered borocyclic ring in DIPYR, but showed none for either α - or γ -DIPYR. In contrast, the geometry calculated for the excited S_1 state does show an out-of-plane distortion in γ -DIPYR ($d_{op} = 0.32 \text{ \AA}$), as well as in DIPYR ($d_{op} = 0.50 \text{ \AA}$), and but virtually none for α -DIPYR ($d_{op} = 0.001 \text{ \AA}$). Out-of-plane distortion of the BF_2 moiety in the α -DIPYR is likely impeded by $\text{H}\cdots\text{F}$ steric conflicts between the nearby protons of the benzannulated ring and the fluorine atoms that lie above and below the molecular plane, as evidenced by through-space coupling of ^1H to ^{19}F in the NMR studies discussed previously. The separation between these atoms are calculated to be 2.36 \AA , which places them 0.4 \AA closer than the sum of their Van der Waal radii. Moreover, energies calculated for out-of-plane vibrations of the boron atom and flanking aromatic rings range between $70\text{--}225 \text{ cm}^{-1}$, similar to values found in BODIPY.³⁴ Therefore, the extremely narrow linewidth for the 0-0 transition of α -DIPYR in methylcyclohexane is likely due to inhibition of out-of-plane vibronic motions of the BF_2 group.



The nodal characteristics for the frontier orbitals of DIPYR are compared here with BODIPY as they share distinct similarities and differences (Figure 5). In an idealized planar BODIPY (C_{2v} point group), the HOMO and LUMO+1 have a_2 symmetry whereas the LUMO is b_1 . Hence, both the HOMO and LUMO+1 have a node that lies on the C_2 axis of the molecule, whereas the LUMO has a substantial atomic orbital density at the *meso* carbon atom. The same symmetric configuration appears in DIPYR; however, the exchange of pyridyl for pyrrole moieties shifts the orbital relationship, such that the HOMO-1 and LUMO are now b_1 symmetry and the HOMO is a_2 . This change in electronic structure leads to a large atomic orbital contribution localized at the *meso* position of the HOMO in DIPYR. However, despite these differences in orbital symmetry

1
2
3 labels, the HOMO–LUMO transition dipole moment in *both* molecules is polarized along the
4
5 long axis of the molecule, perpendicular to the permanent dipole oriented along the short (C_2)
6
7 axis. It is this orthogonal arrangement of (long) transition and (short) permanent dipole moments
8
9 that leads to a high molar absorptivity that is relatively insensitive to solvent polarity in both
10
11 molecules.³⁵
12
13

14
15
16 In addition, it is worth noting that the nodal characteristics of the top half of DIPYR are
17
18 identical to those of the C_7H_9 cation. This orbital pattern, where nodes bisect every other carbon
19
20 atom in the HOMO and LUMO, is a feature common to non-alternant hydrocarbons and leads to
21
22 intense, narrow absorption bands in chromophores such as cyanine dyes.³⁶
23
24

25
26 The relative energies calculated for the valence orbitals are in good agreement with the
27
28 electrochemical oxidation and reduction potentials. The calculated energies for the HOMO and
29
30 LUMO in DIPYR are destabilized by approximately 1.1 eV and 1.3 eV, respectively, compared
31
32 to the energies for the corresponding orbitals in BODIPY. Likewise, HOMO and LUMO
33
34 energies calculated for α - and γ -DIPYR reflect the relative stabilization of these orbital
35
36 determined from their corresponding redox potentials (for α -DIPYR: HOMO = -5.00 eV, LUMO
37
38 = -1.96 eV; for γ -DIPYR: HOMO = -5.01 eV, LUMO = -1.91 eV). Although extension of the π -
39
40 system in chromophores by benzannulation is typically understood to induce a bathochromic
41
42 shift of the absorption and emission bands, the location of benzannulation plays a key role in
43
44 modulating this effect (Hanson's Rules).³⁷ Compared to DIPYR, the decrease in the HOMO–
45
46 LUMO energy gap for α - and γ -DIPYR (0.31 eV and 0.35 eV, respectively) corresponds to the
47
48 respective red-shifts of 0.20 eV (34 nm) and 0.10 eV (19 nm) in their E_{0-0} energies for the S_1
49
50 state.
51
52
53
54
55
56
57
58
59
60

Table 3. Calculated (DFT: B3LYP/6-31G**) and experimental state energies in DIPYR dyes in nm (eV).

	S ₂ calc*	S ₁ calc*	S ₁ exp	T ₂ calc	T ₁ calc	T ₁ exp
DIPYR	451 (2.75) <i>f</i> = 0.029	461 (2.69) <i>f</i> = 0.232	482 (2.57)	511 (2.43)	587 (2.11)	577 (2.15)
α-DIPYR	444 (2.79) <i>f</i> = 0.030	533 (2.33) <i>f</i> = 0.463	524 (2.37)	480 (2.58)	668 (1.86)	638 (1.94)
γ-DIPYR	415 (2.99) <i>f</i> = 0.030	515 (2.41) <i>f</i> = 0.590	504 (2.46)	450 (2.76)	658 (1.89)	626 (1.98)
*Calculated singlet energies were corrected by subtracting 0.44 eV from the computational output.						

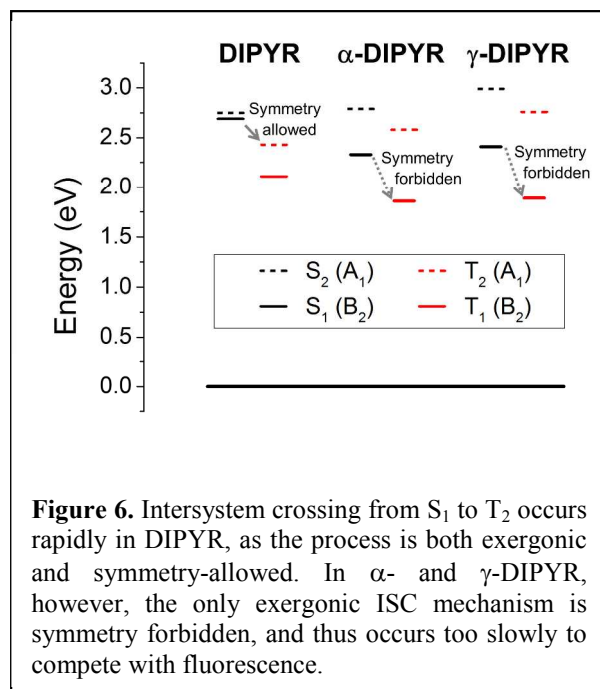
The relative energies of the S₁, S₂ and T₁, T₂ states (Table 3) were calculated for each of the three DIPYR derivatives and evaluated to shed light on the effect of benzannulation in this family of dyes. Both S₀-S₁ and S₀-T₁ transitions are primarily between the HOMO and LUMO, polarized along the long molecular axis, whereas the S₀-S₂ and S₀-T₂ transitions are predominantly between the HOMO and LUMO+1, and polarized along the short axis of the molecules such that they lie parallel to the molecular dipole. Consequently, we can predict that the S₀-S₂ and S₀-T₂ transitions will be stabilized in polar environments. After comparison with experiment, a -0.44 eV shift in energy of was applied to all calculated singlet energies for this family of DIPYR dyes. This seemingly arbitrary correction factor is consistent with the large but linear difference between state energies derived using TD-DFT vs. experimental values in BODIPYs, cyanines and other similar pseudo-aromatic dyes.^{32,33} The discrepancy between experimental and theoretical energies in this case stems from a failure of TD-DFT methods to account for the double-excitation character of singlet states in these systems.³² The correction factor was determined by mean difference between calculated and experimentally observed singlet state energies (S₁, S₂, S₃) across the series. However, the calculated triplet state energies are in relatively good agreement, *i.e.* < 100 mV difference between the calculated and experimental values, as XMCQDPT2 calculations show both triplet states T₁ and T₂ can be

accurately described within the TD-DFT framework due to minimal ($< 1.2\%$) contribution from double excitations (see SI for calculation results).

With the calculated singlet state energies in hand it is possible to explain the observed absorption and emission spectral characteristics for the DIPYR chromophore. DIPYR displays three strong absorption bands in the UV-visible spectrum, corresponding to transitions from the S_0 ground state to the S_1 , S_2 and S_3 states. The S_1 and S_2 states in DIPYR are close enough in energy to have overlapping transition manifolds, with oscillator strength (f) of the S_0 - S_1 transition being roughly an order of magnitude larger than the S_0 - S_2 transition. Thus, the vibronic progression of the S_0 - S_1 absorption band is distorted by the underlying S_0 - S_2 transition. The S_0 - S_2 transition dipole moment is polarized along the short axis of the dye, parallel to the molecular dipole. Therefore, the energy of the S_2 state is expected to be strongly affected in polar media, thereby shifting the wavelength of the S_0 - S_2 transition. In contrast, the S_0 - S_1 transition dipole moment lies along the long axis of the molecule, and as such displays a weak hypsochromic dependence on solvent polarity. The close juxtaposition in energy between the S_1 and S_2 states induces a polarity-dependent relationship in the lineshape of the lowest energy absorption bands in solution as the S_0 - S_2 transition will shift in energy with increasing polarity whereas the S_0 - S_1 transition will remain relatively unchanged (Figure 4). Consequently, the S_0 - S_2 transition will be mixed into the lowest excited state to a greater extent in polar media, evidenced by the relative increase in the 0-1 vibronic feature in the absorption spectrum of DIPYR in polar solvents. This competition between transitions is reflected in the radiative rate constants of DIPYR in methylcyclohexane ($k_r = 9.1 \times 10^7 \text{ s}^{-1}$) versus acetonitrile ($k_r = 5.3 \times 10^7 \text{ s}^{-1}$), where the stabilizing effect of polar solvent increases the contribution from the weaker, dipole-containing S_2 state. In the case of both α - and γ -DIPYR, the S_0 - S_2 transition

does not overlap with the S_0 - S_1 transition, and thus the lineshape of the latter absorption band and radiative rate constants displayed are unchanged upon an increase in solvent polarity.

Another important change brought about by benzannulation is a relative reordering of the S_1 and T_2 state energies. The energy of the T_2 state in DIPYR is calculated to be lower than that of the experimental S_1 state, whereas the energy of the T_2 states calculated for α - and γ -DIPYR are greater than that of the experimental S_1 states, see Figure 6. This difference in ordering between the S_1 and T_2 state energies is due to a stabilization of the LUMO upon benzannulation (ca. -0.50 eV) while the LUMO+1 remains mostly unchanged (-0.15 eV in α -DIPYR and +0.08 eV in γ -DIPYR). The relative ordering of state energies in DIPYR is what leads to the low Φ_{PL} that is further suppressed by an increase in solvent polarity, since ISC from S_1 to T_2 is symmetry allowed and favored by the close proximity in energy between the two states.³⁸ The net result in DIPYR is a fast rate for ISC ($k_{ISC} > 10^9 \text{ s}^{-1}$) that outcompetes radiative decay from the S_1 state. This energetic situation ($T_2 < S_1$) is similar to that present in anthracene and considered responsible for its high rate of intersystem crossing and consequent luminescent efficiency ($k_{ISC} = 10^8 \text{ s}^{-1}$, $\Phi_{PL} = 0.24$).³⁹ In contrast, the higher energy of the T_2 states compared to the S_1 states in α - and γ -DIPYR make ISC to T_2 an endothermic, unfavorable process. Therefore, the only pathway for ISC is directly from S_1 to T_1 , which is symmetry forbidden, and thus a slow process ($k_{ISC} < 10^9 \text{ s}^{-1}$) that results in high Φ_{PL} independent of solvent polarity. Support for this hypothesis is provided by phosphorescence emission experiments. Phosphorescence from DIPYR is readily observed in frozen methyl cyclohexane, whereas more rigorous methods of gated detection and treatment with a heavy atom are needed to observe phosphorescence emission in the benzannulated derivatives, consistent with slow ISC and thus a low yield of T_1 for the latter compounds.



CONCLUSION:

In summary, a small family of simple pyridine-, quinoline-, and isoquinoline-based fluorophores, termed DIPYR dyes, has been characterized and described. The reason for the relatively low Φ_{PL} in the DIPYR parent is the energetic alignment of the T_2 state just below the S_1 state, which leads to relatively efficient intersystem crossing that is competitive with fluorescence, followed by non-radiative decay from the triplet. Benzannulation of the DIPYR moves the T_2 state higher in energy than the S_1 state, thereby leading to a significant decrease in the rate of intersystem crossing and a significant increase in the fluorescent quantum efficiency. The coupling of broad spectral width and high absorption coefficients is promising for generating large carrier densities in organic photovoltaics. There remains significant opportunity for additional manipulation of this library of dyes, in which alkylation, aza- and push-pull substitution, and π -extension are each expected to be useful methods for the modulation of absorption and emission onsets and intensities; a keen understanding of the molecular orbital

characteristics of these compounds will play a major role in color- and intensity-tuning the absorption and emission profiles of new derivatives. We expect that an expanded library of these dyes will serve as a useful tool for fluorescent labelling applications. Further investigation into this class of dyes and their application to light harvesting and energy conversion applications is actively underway.

EXPERIMENTAL:

Instrumentation

UV-visible spectra were recorded on a Hewlett-Packard 4853 diode array spectrometer. Photoluminescence spectra were measured using a QuantaMaster Photon Technology International phosphorescence/fluorescence spectrofluorometer. Quantum yield measurements were carried out using a Hamamatsu C9920 system equipped with a xenon lamp, calibrated integrating sphere and model C10027 photonic multi-channel analyzer (PMA). Photoluminescence lifetimes were measured by time-correlated single-photon counting using an IBH Fluorocube instrument equipped with an LED excitation source. Molar extinction coefficients were obtained by plotting solutions at four concentrations between 0.1 and 0.9 on a Beer's Law plot, with y-intercept set to zero. Line fitting for all samples provided R^2 values greater than 0.98. Excitation, emission, photoluminescence quantum yield, and lifetime measurements were acquired from solutions at maximum optical densities between 0.1-0.2 to minimize the effects of solute-solute interactions. Room temperature photophysical measurements were recorded in methylcyclohexane or acetonitrile and cryogenic photophysical measurements were carried out in methylcyclohexane at 77 K. Methyl iodide was added to α -DIPYR and γ -DIPYR to enhance the rate of ISC in order to observe phosphorescence emission. Reported phosphorescence spectra were acquired in methylcyclohexane at 77 K using a gated

emission scan with 30 μ s delay. NMR spectra were recorded on a Varian 400 NMR spectrometer and referenced to the residual proton resonance of chloroform (CDCl_3) solvent at 7.26 ppm. Matrix assisted laser desorption/ionization (MALDI) mass spectroscopy data was acquired on a Bruker Autoflex Speed LRF.

Computational Methods

All calculations were performed using Jaguar 8.4 (release 12) software package on the Schrodinger Material Science Suite (v2016-2). Gas phase geometry optimizations were calculated using CAM-B3LYP functional with the 6-31G** basis set as implemented in Jaguar. We also employed the extended multiconfigurational quasi-degenerate second order perturbation theory⁴⁰ (XMCQDPT2) method implemented in the Firefly quantum chemistry package⁴¹ to incorporate dynamic correlation to the CASSCF calculations.

General Synthesis

All reagents were purchased from Sigma Aldrich and used without purification. Anhydrous 1,2-dichloroethane was purchased from EMD Millipore.

A 15 mM solution of diheteroarylmethane ligand in dry 1,2-dichloroethane was prepared in an N_2 -purged schlenk flask equipped with a magnetic stir bar and fitted with a reflux condenser. The flask was submerged in a preheated oil bath and brought to reflux, at which time 2.0 eq. boron trifluoride diethyl etherate were added dropwise, causing the color to change from deep yellow to an opaque, pale yellow, corresponding to the rapid formation of precipitate. The solution was stirred for 2 hours at reflux, then cooled to room temperature and treated with 5 eq. N,N -diisopropylethylamine, causing the precipitate to dissolve and the solution to turn deep yellow-orange with a bright green fluorescence. The solution was washed with water and the

aqueous layer was separated and extracted three times with dichloromethane. The organic layers were combined, dried over sodium sulfate, filtered, and reduced to a bright orange polycrystalline solid by rotary evaporation. The products were purified by silica gel flash chromatography with the eluent 30% dichloromethane in hexanes, followed by recrystallization. Single crystal X-ray quality crystals were obtained for DIPYR and γ -DIPYR by recrystallization from the slow diffusion of hexanes into a concentrated dichloromethane solution. Single crystals of α -DIPYR were obtained by very slow cooling (in a dewar) of a concentrated hot methanol solution to -48 °C for 72 hours.

DIPYR: 2.54g (38%) yield. Orange crystals with green reflectance. ^1H NMR (400 MHz, CDCl_3) δ 7.94–7.86 (br. d, 2H, J = 5.5 Hz), 7.25 (ddd, J = 8.9, 6.7, 1.6, 2H), 6.82 (d, J = 8.8 Hz, 2H), 6.50 (dd, J = 6.7, 1.2 Hz, 2H), 5.36 (s, 1H). $^{13}\text{C}\{^1\text{H}\}$ NMR (101 MHz, CDCl_3) δ 149.3, 136.8, 135.6, 121.2, 111.4, 111.4, 85.3. Spectra match those reported in the literature.¹⁷ MS (MALDI) m/z calcd for $\text{C}_{11}\text{H}_9\text{BF}_2\text{N}_2^+$ 218.083 $[\text{M}]^+$; found 217.906.

α -DIPYR: 0.27 g (39%) yield. Orange crystals with green reflectance. ^1H NMR (400 MHz, CDCl_3) δ 8.57 (dt, J = 8.8, 3.5 Hz, 2H), 7.64–7.54 (m, 4H), 7.51 (dd, J = 7.8, 1.5 Hz, 2H), 7.32–7.26 (m, 2H), 6.85 (d, J = 9.0 Hz, 2H), 5.48 (s, 1H). $^{13}\text{C}\{^1\text{H}\}$ NMR (101 MHz, CDCl_3) δ 149.7, 139.8, 136.5, 130.8, 128.1, 124.8, 123.8, 121.9, 121.4 (t, J = 8.3 Hz), 91.5. Anal. Calcd for $\text{C}_{19}\text{H}_{13}\text{BF}_2\text{N}_2$: C, 71.73; H, 4.12; N, 8.81. Found: C, 71.35; H, 4.24; N, 8.55. A melting temperature determination was attempted, but sublimation was observed at atmospheric pressure in the capillary tube at 217 °C. MS (MALDI) m/z calcd for $\text{C}_{19}\text{H}_{13}\text{BF}_2\text{N}_2^+$ 318.114 $[\text{M}]^+$; found 317.999.

γ -DIPYR: 0.84 g (36%) yield. Red-orange crystals with green reflectance. ^1H NMR (400 MHz, CDCl_3) δ 8.37 (d, $J = 7.8$ Hz, 2H), 7.91–7.85 (br. d, $J = 7.0$ Hz, 2H), 7.68 (ddd, $J = 8.0, 6.8, 1.2$ Hz, 2H), 7.64–7.56 (m, 4H), 7.16 (s, 1H), 6.97–6.92 (br. d, $J = 7.1$ Hz, 2H). $^{13}\text{C}\{^1\text{H}\}$ NMR (101 MHz, CDCl_3) δ 148.6, 135.1, 131.7, 130.9, 127.6, 127.0, 124.9, 124.7, 112.1, 81.4. Anal. Calcd for $\text{C}_{19}\text{H}_{13}\text{BF}_2\text{N}_2$: C, 71.73; H, 4.12; N, 8.81. Found: C, 71.57; H, 4.16; N, 8.57. A melting temperature determination was attempted, but sublimation was observed at atmospheric pressure in the capillary tube at 258 °C. MS (MALDI) m/z calcd for $\text{C}_{19}\text{H}_{13}\text{BF}_2\text{N}_2^+$ 318.114 $[\text{M}]^+$; found 318.010.

Supporting Information:

Full NMR spectra, cyclic voltammograms, TD-DFT data and figures, ligand synthesis and absorption and emission spectra, as well as X-ray crystallographic data are available in the supporting information. This material is available free of charge via the Internet at <http://pubs.acs.org>.

Author Information:

Corresponding Author: met@usc.edu

The authors declare no competing financial interest.

Acknowledgements:

Financial support from the Office of Basic Energy Sciences at the Department of Energy (DE-SC0016450) is gratefully acknowledged. We thank Dr. Ralf Haiges for help in refining the crystal structures.

REFERENCES:

- (1) Kurata, S.; Kanagawa, T.; Yamada, K.; Torimura, M.; Yokomaku, T.; Kamagata, Y.; Kurane, R. *Nucleic Acids Res.* **2001**, *29*, e34.
- (2) Li, X.; Traganos, F.; Melamed, M. R.; Darzynkiewicz, Z. *Cytometry* **1995**, *20*, 172-180.
- (3) Meng, Q.; Kim, D. H.; Bai, X.; Bi, L.; Turro, N. J.; Ju, J. *J. Org. Chem.* **2006**, *71*, 3248-3252.
- (4) Metzker, M. L.; Lu, J.; Gibbs, R. A. *Science* **1996**, *271*, 1420-1422.
- (5) Karolin, J.; Johansson, L. B. A.; Strandberg, L.; Ny, T. *J. Am. Chem. Soc.* **1994**, *116*, 7801-7806.
- (6) Sunahara, H.; Urano, Y.; Kojima, H.; Nagano, T. *J. Am. Chem. Soc.* **2007**, *129*, 5597-5604.
- (7) Baruah, M.; Qin, W.; Basarić, N.; De Borggraeve, W. M.; Boens, N. *J. Org. Chem.* **2005**, *70*, 4152-4157.
- (8) Qi, X.; Jun, E. J.; Xu, L.; Kim, S.-J.; Joong Hong, J. S.; Yoon, Y. J.; Yoon, J. *J. Org. Chem.* **2006**, *71*, 2881-2884.
- (9) Zhang, D.; Martin, V.; Garcia-Moreno, I.; Costela, A.; Perez-Ojeda, M. E.; Xiao, Y. *PCCP* **2011**, *13*, 13026-13033.
- (10) Chen, J. J.; Conron, S. M.; Erwin, P.; Dimitriou, M.; McAlahney, K.; Thompson, M. E. *ACS Appl. Mater. Interfaces* **2015**, *7*, 662-669.
- (11) Erten-Ela, S.; Yilmaz, M. D.; Icli, B.; Dede, Y.; Icli, S.; Akkaya, E. U. *Org. Lett.* **2008**, *10*, 3299-3302.
- (12) Hendrickson, H. S.; Hendrickson, E. K.; Johnson, I. D.; Farber, S. A. *Anal. Biochem.* **1999**, *276*, 27-35.
- (13) Loudet, A.; Burgess, K. *Chem. Rev.* **2007**, *107*, 4891-4932.
- (14) Arroyo, I. J.; Hu, R.; Merino, G.; Tang, B. Z.; Peña-Cabrera, E. *J. Org. Chem.* **2009**, *74*, 5719-5722.
- (15) Schmitt, A.; Hinkeldey, B.; Wild, M.; Jung, G. *J. Fluoresc.* **2009**, *19*, 755-758.
- (16) Tram, K.; Yan, H.; Jenkins, H. A.; Vassiliev, S.; Bruce, D. *Dyes Pigm.* **2009**, *82*, 392-395.
- (17) Douglass, J. E.; Barelski, P. M.; Blankenship, R. M. *J. Heterocycl. Chem.* **1973**, *10*, 255-257.
- (18) Sathyamoorthi, G.; Soong, M.-L.; Ross, T. W.; Boyer, J. H. *Heteroat. Chem* **1993**, *4*, 603-608.
- (19) Kubota, Y.; Tsuzuki, T.; Funabiki, K.; Ebihara, M.; Matsui, M. *Org. Lett.* **2010**, *12*, 4010-4013.
- (20) Dyker, G.; Muth, O. *Eur. J. Org. Chem.* **2004**, *2004*, 4319-4322.
- (21) Stephens, D. E.; Nguyen, V. T.; Chhetri, B.; Clark, E. R.; Arman, H. D.; Larionov, O. V. *Org. Lett.* **2016**, *18*, 5808-5811.
- (22) Cruickshank, D. W. J.; Sparks, R. A. *Proc. R. Soc. Lond. A. Math. Phys. Sci.* **1960**, *258*, 270.
- (23) Bondi, A. *J. Phys. Chem.* **1964**, *68*, 441-451.
- (24) Hierso, J. C. *Chem. Rev.* **2014**, *114*, 4838-4867.
- (25) Parton, R. L.; Lenhard, J. R. *J. Org. Chem.* **1990**, *55*, 49-57.
- (26) Lenhard, J. R.; Parton, R. L. *J. Am. Chem. Soc.* **1987**, *109*, 5808-5813.
- (27) Lenhard, J. R.; Cameron, A. D. *J. Phys. Chem.* **1993**, *97*, 4916-4925.
- (28) Nepomnyashchii, A. B.; Bröring, M.; Ahrens, J.; Bard, A. J. *J. Am. Chem. Soc.* **2011**, *133*, 19498-19504.
- (29) Benniston, A. C.; Harriman, A.; Whittle, V. L.; Zelzer, M.; Harrington, R. W.; Clegg, W. *Photochem. Photobiol. Sci.* **2010**, *9*, 1009-1017.
- (30) Nepomnyashchii, A. B.; Bard, A. J. *Acc. Chem. Res.* **2012**, *45*, 1844-1853.

- (31) Granovsky, A. A. *J Chem. Phys.* **2011**, *134*.
- (32) Momeni, M. R.; Brown, A. *J. Chem. Theory Comput.* **2015**, *11*, 2619-2632.
- (33) Charaf-Eddin, A.; Le Guennic, B.; Jacquemin, D. *RSC Adv.* **2014**, *4*, 49449-49456.
- (34) Stromeck-Faderl, A.; Pentlehner, D.; Kensy, U.; Dick, B. *ChemPhysChem* **2011**, *12*, 1969-1980.
- (35) Bergström, F.; Mikhalyov, I.; Hägglöf, P.; Wortmann, R.; Ny, T.; Johansson, L. B. Å. *J. Am. Chem. Soc.* **2002**, *124*, 196-204.
- (36) Dähne, S. *Science* **1978**, *199*, 1163.
- (37) Hanson, K.; Roskop, L.; Djurovich, P. I.; Zahariev, F.; Gordon, M. S.; Thompson, M. E. *J. Am. Chem. Soc.* **2010**, *132*, 16247-16255.
- (38) Nijegorodov, N.; Winkoun, D. P. *Spectrochim. Acta Mol. Biomol. Spectrosc.* **1997**, *53*, 2013-2022.
- (39) Turro, N. J. R., V.; Scaiano, J. C. *Principles of Molecular Photochemistry: An Introduction*; University Science Books: Sausalito, California, USA, 2009.
- (40) Granovsky, A. A. *J. Chem. Phys.* **2011**, *134*, 214113.
- (41) Granovsky, A. A.; Vol. Firefly version 8, p
<http://classic.chem.msu.su/gran/firefly/index.html>.